Optimal control law for multiconjugate adaptive optics

Le Roux B.[1], Conan J.-M.[1], Kulcsar C.[2], Raynaud H.-F.[2],
Mugnier L.M.[1],Fusco T.[1]

[1] Office National d'Etudes et de Recherches Aérospatiales (ONERA),
Châtillon, France
[2] Université Paris 13, Institut Galilée, L2TI,
Villetaneuse, France

ABSTRACT

We propose in this paper an optimal closed loop control law for multiconjugate adaptive optics [MCAO], based on a Kalman filter and a feedback control. The so-called open loop optimal phase reconstruction is recalled. It is based on a Maximum A Posteriori [MAP] approach. This approach takes into account wavefront sensing noise and also makes use of a turbulence profile model and Kolmogorov statistics. We propose a closed-loop modelization via a state-space representation. A Kalman filter is used for the phase reconstruction. This approach is a closed loop generalization of the MAP open loop estimator. It uses the same spatial prior in addition with a temporal model of the turbulence. Results are compared with the Optimized Modal Gain Integrator approach in the classical adaptive optics case and in an MCAO-like case.

Keywords: Multiconjugate Adaptive Optics, Optimal Reconstruction, Closed Loop, Kalman Filter.

1. INTRODUCTION

High resolution imaging with ground-based telescopes is now possible with adaptive optics [AO]. However, classical adaptive optics [AO], using a single deformable mirror [DM] in the pupil, provides a limited corrected field of view [FOV]. Large FOV correction can be obtained by correcting the turbulence volume above the telescope, with several DMs optically conjugated at various altitudes and several guide stars [GSs] for wavefront sensing [WFS]. This corresponds to the multi-conjugate adaptive optics [MCAO] concept. The MCAO concept has been first proposed by Dicke [1] and again in the early 90s with papers of Beckers [2], Tallon [3] and Ellerbroek [4]. It came back recently into fashion with a very impressive number of MCAO papers published, which all show the high potentiality of this technique [5–11] .

One key issue in such a system is the estimation of the correction phases from the wavefront sensing data. Considering an ideal open loop system, we recently proposed an optimal reconstruction method [6] which is briefly recalled here in Sect. 2. It ensures a minimum residual phase variance over a given FOV of interest which means an optimal image quality in this field, using spatial priors. We propose in this article a generalization of this approach for closed loop operation, using a state-space model formalism and based on a Kalman filter and a feedback control. We compare the results obtained with this approach to those obtained with the Optimized Modal Gain Integrator [OMGI] approach in classical AO and in an MCAO-like case.

2. OPTIMAL RECONSTRUCTION IN OPEN LOOP

We call here open loop the ideal case of a system without any delay and where the sensors directly measure the turbulent phase (and not a residual phase). This approach takes no temporal considerations into account.

We consider N_{gs} GSs in the β_i directions. The interest directions, where the correction has to be optimized, are noted α_i. For each WFS direction, we assume that the measurements can be expressed as

$$\phi_{\beta_i}^{mes} = \phi_{\beta_i}^{pup} + \mathbf{w}, \tag{1}$$

Further informations : Email: leroux@onera.fr; URL:http://www.onera.fr/;Phone +33146 734759; Fax +33146 734171

Adaptive Optical System Technologies II, Peter L. Wizinowich, Domenico Bonaccini, Editors, Proceedings of SPIE Vol. 4839 (2003) © 2003 SPIE · 0277-786X/03/$15.00

with w the measurement noise. For the sake of simplicity, we implicitly assume that we directly measure phase and not a derivative of the phase. Otherwise a matrix D describing the WFS process can easily be added in the equation.

The turbulent phase on the telescope pupil is given by the sum of all the turbulent layer contributions:

$$\phi^{tur}_{\beta_i} = \sum_{j=1}^{N_t} \varphi^{tur}_j(\mathbf{r} + h_j.\beta_i) \tag{2}$$

and ϕ^{cor} is also defined as:

$$\phi^{cor}_{\beta_i} = \sum_{j=1}^{N_{DM}} \varphi^{cor}_j(\mathbf{r} + h_j.\beta_i), \tag{3}$$

then, Eq. 1 can be rewritten as :

$$\phi^{mes}_{\beta_i} = \sum_{j=1}^{N_t} \varphi^{tur}_j(\mathbf{r} + h_j.\beta_i) + \mathbf{w}(\mathbf{r}), \tag{4}$$

where φ_j is the phase on the j^{th} layer and N_t is the total number of layers.

We note $\mathbf{M}^{N_t}_{\boldsymbol{\beta}}$ and $\mathbf{M}^{N_t}_{\boldsymbol{\alpha}}$ the matrices which perform the sum of the contributions of each wavefront $\varphi_j(\boldsymbol{\rho}_j)$ in the directions $\boldsymbol{\alpha}$ and $\boldsymbol{\beta}$. $\mathbf{M}^{N_{DM}}_{\boldsymbol{\alpha}}$ and $\mathbf{M}^{N_t}_{\boldsymbol{\alpha}}$ perform the sum of the contributions of each mirror in the directions $\boldsymbol{\alpha}$ and $\boldsymbol{\beta}$. For example, Eq. (2) can be written:

$$\phi^{tur}_{\beta_i} = \mathbf{M}^{N_t}_{\beta_i}.\varphi^{tur}_j(\mathbf{r} + h_j.\beta_i) \tag{5}$$

The reconstruction consists in estimating the correction phases $\{\phi_{cor,k}\}$ from all these measurements $\left\{\phi^{mes}_{\beta_i}\right\}_{gs}$ considering N_{DM} DMs located at different heights h_k ($k \in [1, N_{DM}]$). We call here "optimal reconstruction" a reconstruction that ensures a minimum mean residual variance in the FOV of interest, that is the best image quality on this field of view. The criterion to be minimized therefore reads:

$$\boldsymbol{\epsilon} = \int_{\{\alpha\}_{fov}} \left\langle \left\| \phi^{tur}_{pup}(\mathbf{r}, \boldsymbol{\alpha}) - \phi^{cor}_{pup}(\mathbf{r}, \boldsymbol{\alpha}) \right\|^2 \right\rangle_{\varphi, noise} d\boldsymbol{\alpha}, \tag{6}$$

where $\|.\|^2$ denotes the spatial variance in the telescope pupil. ϕ_{cor} is the sum of the correction phases $\{\varphi_{cor,k}\}$ which are assumed to be some function of the WFS data. We therefore look for such a function so as to minimize the criterion, in average over turbulence and noise outcomes as stated by the notation: $\langle . \rangle_{\varphi, noise}$. This implies some statistical knowledge on noise and turbulence.

When assuming Gaussian statistics for noise and turbulence, the minimization of this criterion leads to a solution in $\boldsymbol{\varphi}^{cor} = \{\varphi_{cor,k}\}_{DM}$ which is linear with respect to the wavefront measurements. The solution can be written in this simple form [6]:

$$\boldsymbol{\varphi}^{cor} = \mathbf{P}_{[\{\boldsymbol{\alpha}\}_{fov}; DM]} \cdot \mathbf{W}_{tomo} \cdot \left\{\phi^{mes}_{\beta_i}\right\}_{gs} \tag{7}$$

$$= \mathbf{P}_{[\{\boldsymbol{\alpha}\}_{fov}; DM]} \cdot \mathbf{W}_{tomo} \cdot \boldsymbol{\Phi}^{mes}_{\boldsymbol{\beta}}, \tag{8}$$

with

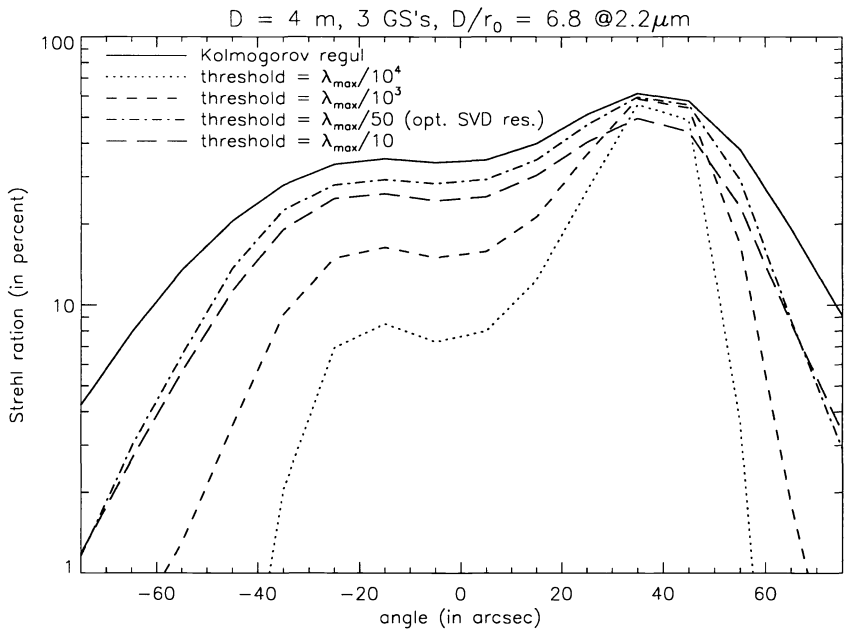

Figure 1. Comparison between the Kolmogorov regularized MAP approach [solid line] and a truncated SVD restoration using different truncation thresholds. The Strehl Ratio versus the FOV position is plotted.

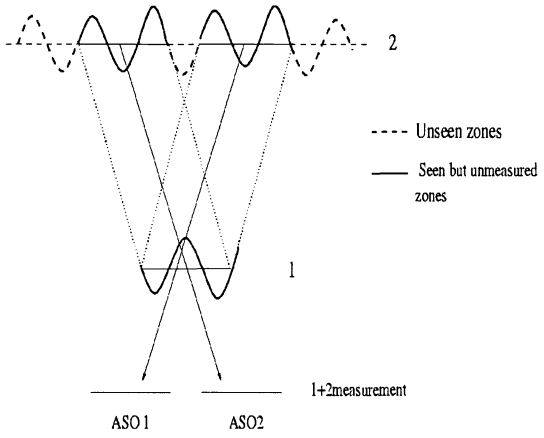

Figure 2. Illustration of the concept of unseen modes.

unseen mode is a mode that can't be distinguished by the sensors from some others [13]. An example of unseen modes in MCAO is shown in Fig. (2). The phase on the low altitude layer (high energy) can't be distinguished from the high altitude layer phase. In the TSVD approach, those modes are filtered out. The more the unseen modes contain energy and the more the loss of performance is important. In the optimal approach, the use of spatial priors allows to partially recover these unseen modes.

$$\mathbf{W}_{tomo} = \Sigma_{\varphi} \left(\mathbf{M}_{N_{gs}}^{N_t}\right)^T \left(\mathbf{M}_{N_{gs}}^{N_t} \Sigma_{\varphi} \left(\mathbf{M}_{N_{gs}}^{N_t}\right)^T + \Sigma_{\mathbf{w}}\right)^{-1} \tag{9}$$

and

$$\mathbf{P}_{[\{\boldsymbol{\alpha}\}_{fov};DM]} = \left(\int_{\{\boldsymbol{\alpha}\}_{fov}} \left(\mathbf{M}_{\boldsymbol{\alpha}}^{N_{DM}}\right)^T \mathbf{M}_{\boldsymbol{\alpha}}^{N_{DM}} d\boldsymbol{\alpha}\right)^+ \left(\int_{\{\boldsymbol{\alpha}\}_{fov}} \left(\mathbf{M}_{\boldsymbol{\alpha}}^{N_{DM}}\right)^T \mathbf{M}_{\boldsymbol{\alpha}}^{N_t} d\boldsymbol{\alpha}\right), \tag{10}$$

with Σ_{φ} and $\Sigma_{\mathbf{w}}$ the covariance matrices of the phase and the noise. $\mathbf{M}_{N_{gs}}^{N_t}$ is defined as

$$\mathbf{M}_{N_{gs}}^{N_t} = \left(\mathbf{M}_{\beta_1}^{N_t}, \ldots, \mathbf{M}_{\beta_i}^{N_t}, \ldots, \mathbf{M}_{\beta_{N_{gs}}}^{N_t}\right). \tag{11}$$

The optimal reconstruction can be seen as a two step process. The first step corresponding to $\mathbf{W}_{tomo}$ gives an optimal estimation of the turbulent phases $\{\varphi_j\}$ on each layer. This reconstruction is often called tomographic since it gives a reconstruction of the turbulent volume from the projections given by the WFSs. It takes into account the GS geometry, the WFS measurement model, the noise and turbulence statistics. Both noise and turbulence are characterized by their covariance matrix. Concerning turbulence we assume independent layers with Kolmogorov statistics and we use a C_n^2 profile. Note that $\mathbf{W}_{tomo}$ is not related to the DMs and is independent of the FOV of interest. The second step corresponding to $\mathbf{P}_{[\{\boldsymbol{\alpha}\}_{fov};DM]}$ consists in a projection of the tomographic solution onto the DMs to obtain the correction phases $\{\varphi_{cor,k}\}$ which optimizes the correction in the desired FOV. It is a geometrical operation which gives the correction phases from the phase in the volume. It only depends on the number and position of the DMs with respect to the true layers, and on the FOV of interest.

A cruder approach, which is often used to inverse this ill-posed problem of the phase correction estimation in each DM, consists in using a least square minimization [12], that is to consider a truncated singular value decomposition [TSVD]. With our notations, this wavefront estimator is therefore given by the well-known following relation:

$$\boldsymbol{\varphi}^{cor} = \left(\left(\mathbf{M}_{N_{gs}}^{N_t}\right)^T \left(\mathbf{M}_{N_{gs}}^{N_t}\right)\right)^+ \left(\mathbf{M}_{N_{gs}}^{N_t}\right)^T \boldsymbol{\Phi}_{\boldsymbol{\beta}}^{mes}, \tag{12}$$

where $\mathbf{M}_{N_{gs}}^{N_t}$ is the interaction matrix between the DMs and the WFSs. Because $\left(\mathbf{M}_{N_{gs}}^{N_t}\right)^T \left(\mathbf{M}_{N_{gs}}^{N_t}\right)$ is an ill-conditioned matrix , the inversion is made using a singular value decomposition (SVD) in which the lower modes values are set to zero in order to avoid the noise amplification.

For illustration, we show in Fig. (1) a two DM, three GS case extracted from the reference [6]. The three GSs used for WFS are located at the vertices of an equilateral triangle with a separation of 70 arcsec, the DMs are located at 1.25 and 6.25 km, $D/r_o = 6.8$ at the observing wavelength (r_o is the Fried parameter). The graph represents the Strehl Ratio along a line joining the center of the GSs triangle and one GS, for the different estimators. One can see, as expected, that the use of a Kolmogorov regularization, where Σ_{φ} is computed assuming that all the turbulence is equally distributed on the two DMs gives better results than the classical truncated SVD (Equation 12) whatever the chosen truncation threshold (note that the "optimal" choice of this threshold is one of the major problem of the SVD approach). For the optimal SVD threshold ($\lambda_{max}/50$ here), only 72 modes are corrected from the available 199 modes of the system (the piston is not considered).

There are essentially two reasons why the MAP is better than the TSVD approach. The first one is the automatic minimization of noise propagation (no ad-hoc threshold to be adjusted). The second fundamental reason why the MAP optimal approach is better in MCAO is the presence of "unseen modes". What we call

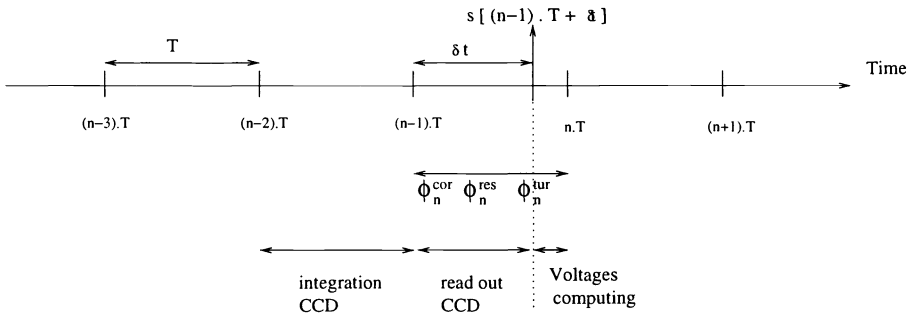

Figure 3. Temporal diagram showing the different time intervals.

3. OPTIMAL CONTROL LAW FOR CLOSED LOOP OPERATION

3.1. Notations, definition of the problem and basic relations

The measurement is obtained with an exposure time T and the correction $\boldsymbol{\varphi}^{cor}(t)$ is constant between $n.T$ and $(n+1).T$. Then the problem can be discretized using T as the sampling period. For any continuous variable $\mathbf{z}(t)$, one can associate the discrete quantity $\mathbf{z}_n$ defined as:

$$\mathbf{z}_n = \frac{1}{T}.\int_{(n-1).T}^{n.T} \mathbf{z}(t).dt. \tag{13}$$

The temporal diagram of the system in Fig. (3) shows how measurements and computations follow one another.

The turbulent phase in all layers $\boldsymbol{\varphi}_n^{tur}$, the correction phase in all mirrors $\boldsymbol{\varphi}_n^{tur}$ and the residual phase in the pupil in the N_{gs} guide star directions $\boldsymbol{\Phi}_n^{res}$ are linked by:

$$\boldsymbol{\Phi}_n^{res} = \mathbf{M}_{N_{gs}}^{N_t}.\boldsymbol{\varphi}_n^{tur} - \mathbf{M}_{N_{gs}}^{N_{DM}}.\boldsymbol{\varphi}_n^{cor}, \tag{14}$$

with $\mathbf{M}_{N_{gs}}^{N_t}$,$\mathbf{M}_{N_{gs}}^{N_{DM}}$ defined as previously.

The residual phase in the N_{gs} guide star directions reads in the slope space:

$$\mathbf{s}_{n+1} = \mathbf{s}[nT + \delta t] = \mathbf{D}.\boldsymbol{\Phi}_n^{res}. \tag{15}$$

$\mathbf{s}(t)$ is the vector of slopes. $\mathbf{D}$ is the interaction matrix between the phase space and the slopes space.

If $\mathbf{u}_n$ is the voltages applied between n and $n+1$:

$$\boldsymbol{\varphi}_n^{cor} = \mathbf{N}.\mathbf{u}_{n-1}, \tag{16}$$

with $\mathbf{N}$ the interaction matrix between the mirror space and the phase space. Vector $\mathbf{u}_n$ is chosen so as to minimize the residual phase in the directions α_i : $||\mathbf{M}_{\boldsymbol{\alpha}}^{N_t}.\boldsymbol{\varphi}_n^{tur} - \mathbf{M}_{\boldsymbol{\alpha}}^{N_{DM}}.\boldsymbol{\varphi}_n^{cor}||^2$.

The measurement obtained at time n is :

$$\mathbf{y}_n = \mathbf{s}[(n-1)T + \delta t] + \mathbf{w}_n, \tag{17}$$

$\mathbf{w}$ a white noise (measurement noise). Its covariance matrix is noted $\Sigma_{\mathbf{w}}$ Then, by using Equations 14, 15 and 16 one can get:

$$\mathbf{y}_n = \mathbf{D}.\left(\mathbf{M}_{N_{gs}}^{N_t}.\boldsymbol{\varphi}_{n-1}^{tur} - \mathbf{M}_{N_{gs}}^{N_{DM}}.N.\mathbf{u}_{n-2}\right) + w_n. \tag{18}$$

The turbulence evolution can be expressed as

$$\varphi_{n+1}^{tur} = F.\left[\varphi_n^{tur}, \varphi_{n-1}^{tur}, \varphi_{n-2}^{tur}, ...\right] + \nu_n. \tag{19}$$

with ν a white noise, of covariance matrix Σ_ν, and F a linear function. For example, the first order model is

$$\varphi_{n+1}^{tur} = A.\varphi_n^{tur} + \nu_n. \tag{20}$$

In this model, Σ_ν can be easily determined : as the global energy must be conserved, $\Sigma_\nu = \Sigma_\varphi - A^T \Sigma_\varphi A$, with Σ_φ the covariance matrix of the phase (Kolmogorov).

With a first order model the temporal correlation function decreases exponentially. Real turbulence temporal evolution [14] can be fitted can be fitted more precisely by using higher order model.

3.2. The linear state space modelization

A linear state space model describes the dynamical behavior of a system and its outputs (measurements) using a state space vector, which evolution is given by a linear equation.

In our case, the state model must summarize Equations 16, 18 and 19 into :

$$\mathbf{X}_{n+1} = \mathbf{A_1}_n.\mathbf{X}_n + \mathbf{A_2}_n.\mathbf{u}_n + \mathbf{V}_n \tag{21}$$

$$\mathbf{y}_n = \mathbf{A_3}_n.\mathbf{X}_n + \mathbf{w}_n. \tag{22}$$

where $\mathbf{V}_n$ and $\mathbf{w}_n$ are Gaussian white noises with covariance matrices $\Sigma_\mathbf{v}$ and $\Sigma_\mathbf{w}$. $\mathbf{X}$ is the state vector, the first equation is the state equation and the second one is the observation equation.

If we consider that the system is stationary, the $\mathbf{A_i}_n$ matrices are time independent, $\mathbf{A_1}_n = \mathbf{A_1}$, $\mathbf{A_2}_n = \mathbf{A_2}$, $\mathbf{A_3}_n = \mathbf{A_3}$.

The choice of the state vector is crucial. $\mathbf{X}$ has to contain all variables necessary to describe the evolution of the system (21) and of the measurements (22). Equation 18 implies then that $\mathbf{X}_n$ contains φ_{n-1}^{tur} and $\mathbf{u}_{n-2}$. The voltages $\mathbf{u}_n$ are determined only through $\mathbf{X}_n$ so as to correct φ_{n+1}^{tur} (this corresponds to a prediction) . This implies that φ_{n+1}^{tur} has to be in $\mathbf{X}_n$. $\mathbf{X}_n$ needs also to contain all the $\varphi_{n_i}^{tur}$ used in Eq. 19.

For a first order evolution model, the state vector is then: $\mathbf{X}_n = \begin{pmatrix} \varphi_{n+1}^{tur} \\ \varphi_n^{tur} \\ \varphi_{n-1}^{tur} \\ \mathbf{u}_{n-1} \\ \mathbf{u}_{n-2} \end{pmatrix}$ and the state model is :

.

$$\mathbf{X}_{n+1} = \begin{pmatrix} \mathbf{A} & 0 & 0 & 0 & 0 \\ Id & 0 & 0 & 0 & 0 \\ 0 & Id & 0 & 0 & 0 \\ 0 & 0 & 0 & 0 & 0 \\ 0 & 0 & 0 & Id & 0 \end{pmatrix}.\mathbf{X}_n + \begin{pmatrix} 0 \\ 0 \\ 0 \\ Id \\ 0 \end{pmatrix}.\mathbf{u}_n + \begin{pmatrix} \nu_n \\ 0 \\ 0 \\ 0 \\ 0 \end{pmatrix} \tag{23}$$

$$\mathbf{y}_n = \mathbf{D}.\begin{pmatrix} 0 & 0 & \mathbf{M}_{N_{gs}}^{N_t} & 0 & -\mathbf{M}_{N_{gs}}^{N_{DM}}.\mathbf{N} \end{pmatrix}.\mathbf{X}_n + \mathbf{w}_n \tag{24}$$

$$\mathbf{z}_n = \begin{pmatrix} 0 & \mathbf{M}_{\boldsymbol{\alpha}}^{N_t} & 0 & -\mathbf{M}_{\boldsymbol{\alpha}}^{N_{DM}}.\mathbf{N} & 0 \end{pmatrix}.\mathbf{X}_n. \tag{25}$$

$\mathbf{z}_n$ is the vector to be controlled. The goal is to minimize $||\mathbf{z}_n||^2$.

3.3. Kalman filter and feedback control

The control loop can be divided in two steps : the estimation and the feedback control.

Once the state model is known, the optimal estimation of $\mathbf{X}_n$ is done by a Kalman filter. It is a recursive estimator, which takes the form:

$$\hat{\mathbf{X}}_{n+1/n} = \mathbf{A_1}.\hat{\mathbf{X}}_{n/n-1} + \mathbf{A_2}.\mathbf{u}_n + \mathbf{A_1}.\mathbf{H}_n.(\mathbf{y}_n - \mathbf{A_3}.\hat{\mathbf{X}}_{n/n-1}), \tag{26}$$

where $\mathbf{X}_{n+1/n}$ is the prediction of $\mathbf{X}_{n+1}$ obtained using $\{\mathbf{Y}_0, ..., \mathbf{Y}_n\}$.

$\mathbf{H}_n$ is called the observator gain and is doing the balance between the *a priori* and the measurements. It is equal to :

$$\mathbf{H_n} = \Sigma_{n/n-1}.{\mathbf{A_3}}^T.\left(\mathbf{A_3}.\Sigma_{n/n-1}.{\mathbf{A_3}}^T + \Sigma_{\mathbf{w}}\right)^{-1}, \tag{27}$$

with $\Sigma_{\mathbf{w}}$ the matrix covariance of the noise and $\Sigma_{\mathbf{n/n-1}}$ the matrix covariance of the state vector estimation error, predicted for the instant n at the instant $n-1$.

$\Sigma_{n/n-1}$ is computed by solving the Ricatti equation :

$$\Sigma_{n+1/n} = \mathbf{A_1}.\Sigma_{n/n-1}.{\mathbf{A_1}}^T + \Sigma_{\mathbf{v}} - \mathbf{A_1}.\Sigma_{n/n-1}.{\mathbf{A_3}}^T.\left(\mathbf{A_3}.\Sigma_{n/n-1}.{\mathbf{A_3}}^T + \Sigma_{\mathbf{w}}\right)^{-1}.\mathbf{A_3}\Sigma_{n/n-1}.{\mathbf{A_1}}^T. \tag{28}$$

Once the estimation of the turbulent phase is done, the voltages are determined by a projection of the estimated phase onto the mirrors so that $\mathbf{z}_n$ is minimum. The projector is the same that the one given in Sect. 2, Eq. 10 :

$$\mathbf{u}_n = \mathbf{P}_{\left[\{\boldsymbol{\alpha}\}_{fov};DM\right]}.\hat{\boldsymbol{\varphi}}^{tur}_{n+1/n}. \tag{29}$$

3.3.1. Closed loop generalization of the open loop MAP approach

The Kalman approach as defined above can be seen as an implementation in closed loop of the MAP approach. One can already note that the estimators are very similar in their form : an estimation phase followed by a projection onto the mirror modes.

Besides one can show that with a zero order evolution model, $\mathbf{A} = 0$ (which only means that the temporal correlation is not used) and no delay (which means that the correction is applied immediately), the Kalman estimator exactly comes down to the open loop estimator given in Eq. (9). In open loop, the prediction for the turbulent phase is 0, because no temporal prior is used. If we write the expression of the estimated (and not predicted) turbulent phase, we obtain:

$$\hat{\boldsymbol{\varphi}}^{tur}_{n/n} = \hat{\boldsymbol{\varphi}}^{tur}_{n/n-1} + \mathbf{H}_n.\left(\mathbf{y}_n - \hat{\mathbf{y}}_{n/n-1}\right). \tag{30}$$

By replacing $\hat{\mathbf{X}}_{\mathbf{n/n-1}}$ and $\hat{\mathbf{y}}_{\mathbf{n/n-1}}$ (the measurement prediction) by 0 and $\mathbf{H_n}$ by its expression given in Eq. (27), one finds indeed the open loop optimal expression already given in Eq. (9).

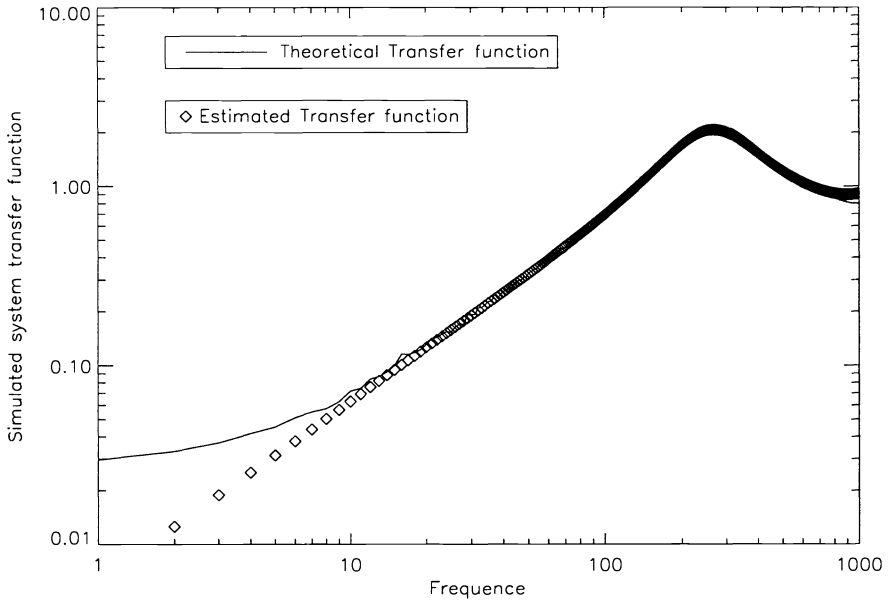

Figure 4. Transfer function of the simulated system.

4. SIMULATIONS, RESULTS AND INTERPRETATIONS

4.1. Simulations conditions

All the simulations presented here are closed loop simulations.

Turbulence simulation conditions:

The turbulent phase is composed of 100 Zernike polynomials. To limit the complexity of the Kalman filter a first order model temporal model will be used. The turbulent wavefront evolution will therefore also be simulated with the first order model presented in Eq. (20) to ensure coherence between the data and the model. To respect the characteristics of turbulence temporal evolution we still enforce a correlation time which decreases with the Zernike number [14]. An equivalent wind speed is deduced from these correlation times. The ratio of the equivalent wind speed and the telescope diameter v/D is equal to 2 Hz, while the sampling frequency is tuned to investigate different cases. D/r_o is set to 10.

System simulation conditions:

We have simulated a classical AO system using the proposed state model. The delay of the loop is two sampling period (as already mentioned and shown in Fig. (3)).

The rejection transfer function in the case of a simple integrator control was estimated from the simulated data by computing :

$$\frac{PSD_{res,wn}}{PSD_{wn}}, \tag{31}$$

where $PSD_{res,wn}$ is the PSD of the residual phase when the turbulent phase is only a white noise and PSD_{wn} is the PSD of this white noise. It is presented in Fig. (4) for a gain of 0.5. The theoretical transfer function [15] is plotted for comparison. This gives a first validation of the simulation procedure. The diameter of the telescope is 8m. The sensor measures directly the 100 Zernike polynomials, meaning that the matrix D is assumed to be identity. The measurement noise is representative of a 9×9 microlenses Shack Hartmann wave front sensor. The Signal to Noise Ratio has been taken between 0 and 50 (the SNR being defined as the variance of the wave

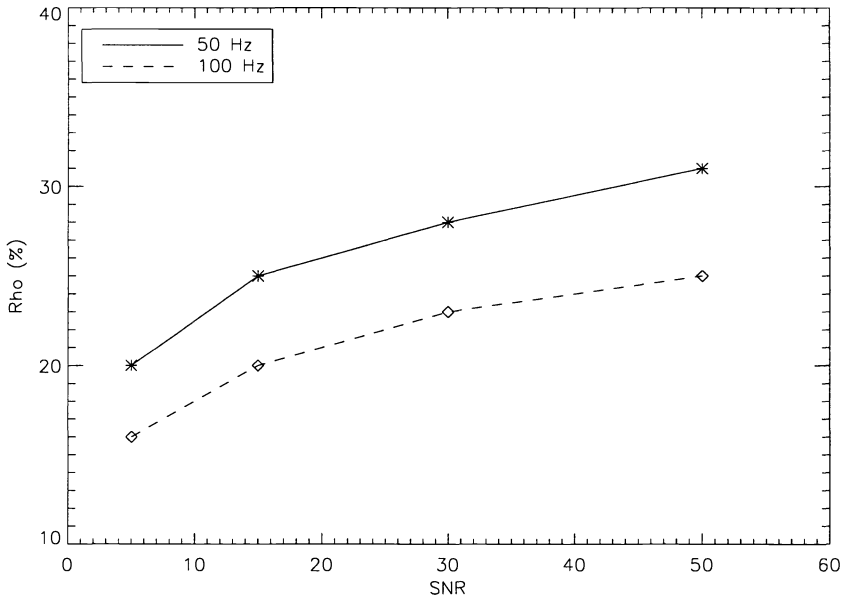

Figure 5. ρ, in %, versus SNR for two sampling frequencies 50Hz and 100Hz.

front sensor measurements under the measurement noise variance). The mirror corrects directly the 100 Zernike polynomials.

4.1.1. Classical AO - Comparison of the Kalman approach to the "Optimized Modal Gain integrator".

The OMGI was proposed in 1994 by E. Gendron [16–18] and is used in classical AO systems (NAOS, for instance [19]). The integrator gains are estimated mode by mode to minimize the residual phase variance. This is done by using the PSD of the turbulent phase, of the noise, and the transfer functions of the system. The higher is the gain, the more the noise is amplified, and the more the temporal evolution of the turbulence phase is taken into account. There is an optimum which is computed and applied.

To compare the two approaches, we have defined the factor ρ, which gives the gain over OMGI obtained by using a Kalman filter. If $\sigma^2_{res}(Kalman)$ and $\sigma^2_{res}(OMGI)$ are the variances of the residual phases obtained with the two methods, the gain is defined as:

$$\rho = 1 - \frac{\sigma^2_{res}(Kalman)}{\sigma^2_{res}(OMGI)}. \tag{32}$$

If $\sigma^2_{res}(Kalman)$ is 0, ρ is 100%. If it is equal to $\sigma^2_{res}(OMGI)$, ρ is equal to 0%.

The comparison has been done with two sampling frequencies : $\frac{1}{T} = 50$ Hz and $\frac{1}{T} = 100$ Hz. Fig. (5) represents the evolution of ρ with the SNR for these two sampling frequencies.

It is easy to understand why the gain with the Kalman approach increases when the sampling frequency decreases. The lower the sampling frequency is low, the more the turbulent phase changes between two measurements and the more we need to make a good prediction. The OMGI contains no prediction, that's why ρ increases when the sampling frequency decreases.

ρ increases with the SNR. Actually, if the SNR tends towards zero, any estimator tends to be equivalent and if the SNR tends towards infinity, the phase estimation is more and more precise and it becomes easier to make a good prediction by using the temporal priors.

The results we obtained can be compared to those shown by C. Dessenne [15, 20] while testing a temporal predictor. Our results have quite a similar behavior as Dessenne's predictor. This shows that the behavior of parameter ρ in Fig. 5 can be well explained by the predictive aspect of the Kalman filter. Furthermore, the knowledge and the optimal use of the noise statistics, the turbulent phase statistics and the temporal correlations of turbulent phase modes allows the Kalman filter to make a better estimation of the turbulent phase. This explains that ours results are slightly better than Dessenne's.

4.1.2. MCAO-like case, introduction of unseen modes and correction of those modes.

The second part of our work consists in a study of the capacity of estimating unseen modes, which is the key point for MCAO systems. We will not simulate a realistic MCAO system but we will only modify our classical AO simulation to demonstrate this capacity on a very simple example.

Previously, the same 100 Zernike polynomials were used to describe the turbulent phase, the measured phase and the correction phase. That means that the interaction matrix $\mathbf{D}$ between the turbulent phase and the measured phase was the identity matrix.

To introduce unseen modes, we have chosen to use a matrix D which mixes two polynomials. More precisely, we consider here that the sensor cannot distinguish Z_4 and Z_{17}, but it only measures the average of the corresponding Zernike coefficients.

If $\{a_i\}$ are the coefficients of the turbulent phase on the Zernike basis, the measurement is then:

$$s_4 = \frac{a_4 + a_{17}}{2}, \tag{33}$$

$$s_{17} = \frac{a_4 + a_{17}}{2}, \tag{34}$$

$$s_i = a_i \quad \text{for i different of 4 and 17} \tag{35}$$

instead of $s_i = a_i$ for all modes, like previously.

With this matrix D we create one unseen mode: $Z_4 - Z_{17}$.

We present in Fig. (6) the variance of the residual phase mode by mode for the Kalman approach and the OMGI approach.

The OMGI filters out the unseen mode and induces an large error on the estimation of both a_4 and a_{17}. The Kalman approach uses spatial priors (Σ_φ and $\Sigma_{\mathbf{w}}$) and temporal priors to estimate those two modes. The result corresponds to what was expected : the advantage to use a Kalman filter in this case is obvious.

We have plotted on the same graphics (Fig. 6) the residual variance for the unseen modes given by the optimal open loop case. It is interesting to compare those results to the performance of the Kalman approach. The comparisons show that the prediction done by the Kalman filter in closed loop tends towards the ideal results obtained in the open loop case. This is quite important because it means that previous results and conclusions given in open loop with the optimal approach in MCAO [5, 21–23], as the optimal number of mirrors, number and geometry of guide stars, field of view and achievable performance, should also be verified in closed loop.

5. CONCLUSION

We have proposed in this paper an optimal closed loop control which can be applied to classical and multiconjugate adaptive optics. It is based on a linear state space model with a Kalman observator. This approach gives a optimal estimation of the turbulence in closed loop. It incorporates both spatial and temporal information on the turbulent phase, as well as information on the noise statistics.

We have shown through a numerical simulation that this approach gives much better results than the usual techniques even in classical AO. We also proved that this approach was very efficient to deal with unseen modes which is an important feature for MCAO operation.

The full simulation of a realistic MCAO system is under progress as well as an experimental validation, in the laboratory, of this new control technique. This approach should be also very promising for very high Strehl ratio AO systems since it can potentially handle efficiently various effects generally limiting AO performance: aliasing, waffle modes, telescope vibrations and system mis-calibrations.

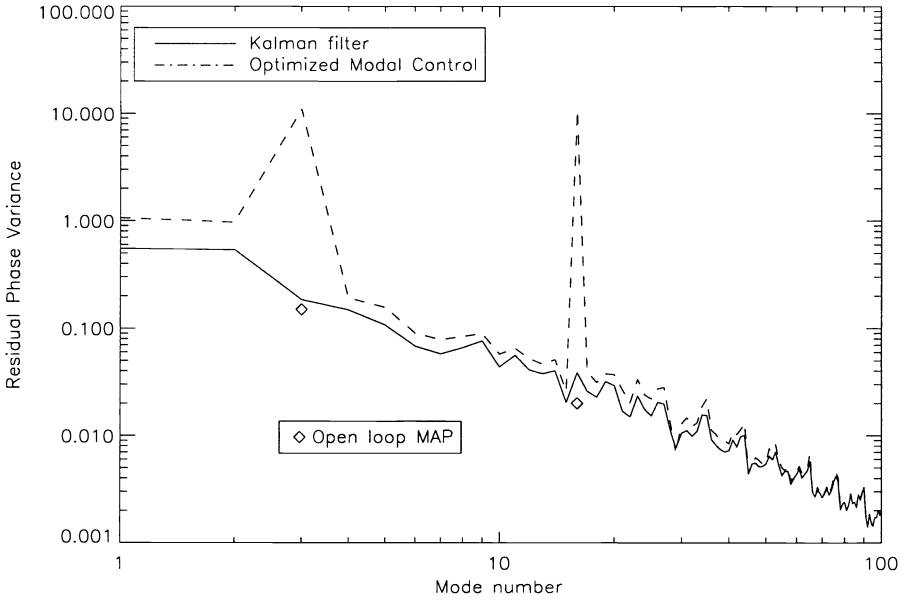

Figure 6. Variance of the residual phase in the MCAO-like case.

REFERENCES

1. R. Dicke, "Phase-contrast detection of telescope seeing and their correction," *Astron. J.* , pp. 605–615, 1975.
2. J. Beckers, "Increasing the size of the isoplanatic patch with multiconjugate adaptive optics.," in *Very Large Telescopes and their Instrumentation*, e. Ulrich, M.-H., ed., *ESO Conference and Workshop Proceedings* **2**, pp. 693–703, 1988.
3. T. M., F. R., and V. J., "3-d wavefront sensing and multiconjugate adaptive optics.," in *Progress in Telescope and Instrumentation Technologies*, e. Ulrich, M.-H., ed., *ESO* **42**, pp. 517–521, 1992.
4. B. L. Ellerbroek, "First-order performance evaluation of adaptive-optics systems for atmospheric-turbulence compensation in extended-field-of-view astronomical telescopes.," J. Opt. Soc. Am. A. **11(2)**, pp. 783–805, 1994.
5. T. Fusco, J.-M. Conan, V. Michau, L. Mugnier, and G. Rousset, "Efficient phase estimation for large field of view adaptive optics.," Opt. Lett. **24(21)**, pp. 1472–1474, 1999.
6. T. Fusco, J.-M. Conan, G. Rousset, L. Mugnier, and V. Michau, "Optimal wavefront reconstruction strategies for multiconjugate adaptive optics.," *J. Opt. Soc. Am. A* **18**, 2001.
7. M. Le Louarn, Étoiles laser pour les grands télescopes : effet de cône et implications astrophysiques,*PhD thesis*, Universitë Lyon I - Claude Bernard., 2000.
8. R. Ragazzoni, E. Marchetti, and F. Rigaut, "Modal tomography for adaptive optics.," Astron. Astrophys. **342**, pp. 53–56, 1999.
9. R. Ragazzoni, "No laser guide stars for adaptive optics in giant telescopes.," Astron. Astrophys. Suppl. Ser. **136**, pp. 205–209, 1999.
10. F. Rigaut, B. L. Ellerbroek, and R. Flicker, "Principles, limitations and performance of multi-conjugate adaptive optics.," in Adaptive Optical Systems Technology, e. Wizinowich, P. L., ed., *Proc. Soc. Photo-Opt. Instrum. Eng.* **4007**, pp. 1022–1031, 2000.
11. A. Tokovinin, M. Le Louarn, and M. Sarazin, "Isoplanatism in multi-conjugate adaptive optics system.," J. Opt. Soc. Am. A **17(10)**, pp. 1819–1827, 2000.

12. R. Flicker, F. Rigaut, and B. Ellerbroek, "Comparison of multiconjugate adaptive optics configurations and control algorithms for the gemini-south 8-m telescope.," *ESO Conference and Workshop Proceedings* **4007**, pp. 1032–1043, 2000.
13. T. Fusco, J.-M. Conan, G. Rousset, and V. Michau, "Performance and limitation of phase estimating algorithms for multiconjugate adaptive optics," *Barcelone*, 2000.
14. J.-M. Conan, G. Rousset, and P.-Y. Madec, "Wave-front temporal spectra in high-resolution imaging through turbulence," **12**, pp. 1559–1570, July 1995.
15. C. Dessenne, *Commande modale et prédictive en optique adaptative classique, PhD thesis*, Université Paris VII, 1998.
16. E. Gendron and P. Lena, "Astronomical adaptive optics i. modal control optimization," *Astronomy and Astrophysics* **291**, pp. 337–347, 1994.
17. E. Gendron and P. Lena, "Astronomical adaptive optics ii. experimental results of an optimize modal control," *Astronomy and Astrophysics* **111**, pp. 153–167, 1994.
18. E. Gendron, *Optimisation de la commande modale en optique adaptative : Application a l'astronomie, Phd thesis*, Université VII, 1995.
19. G. Rousset, F. Lacombe, P. Puget, E. Gendron, R. Arsenault, P. Y. Kern, D. Rabaud, P. Madec, N. N. Hubin, G. Zins, E. Stadler, J. Charton, P. Gigan, and P. Feautrier, "Status of the VLT Nasmyth adaptive optics system (NAOS)," in *Proc. SPIE Vol. 4007, p. 72-81, Adaptive Optical Systems Technology, Peter L. Wizinowich; Ed.*, **4007**, pp. 72–81, 2000.
20. C. Dessenne, P.-Y. Madec, and G. Rousset, "Optimization of a predictive controller for the closed loop adaptive optics," *Appl. Opt.* **37**, p. 4623, 1998.
21. T. Fusco, J.-M. Conan, V. Michau, G. Rousset, and F. Assémat, "Multi-conjugate adaptive optics: Comparison of phase reconstruction approaches for large field of view.," in Optics in Atmospheric Propagation and Adaptive Systems VI, e. In Wizinowich, P. L., ed., *Proc. Soc. Photo-Opt. Instrum. Eng.* **4167**, 2000.
22. T. Fusco, J.-M. Conan, V. Michau, G. Rousset, and L. Mugnier, "Isoplanatic angle and optimal guide star separation for multiconjugate adaptive optics.," in Adaptive Optical Systems Technology, e. In Wizinowich, P., ed., *Proc. Soc. Photo-Opt. Instrum. Eng.* **4007**, pp. 1044–1055, 2000.
23. T. Fusco, *Correction partielle et anisoplanetisme en Optique Adaptative : traitements a posteriori et Optique Adaptative Multiconjuguée, Phd thesis*, Université de Nice Sophia-Antipolis, 2000.